Molecular Cancer Therapeutics

AZD6738, A Novel Oral Inhibitor of ATR, Induces Synthetic Lethality with ATM Deficiency in Gastric Cancer Cells

Ahrum Min[1,2], Seock-Ah Im[1,2,3], Hyemin Jang[1], Seongyeong Kim[1], Miso Lee[1], Debora Keunyoung Kim[4], Yaewon Yang[1,3], Hee-Jun Kim[1,5], Kyung-Hun Lee[1,2,3], Jin Won Kim[1,6], Tae-Yong Kim[1,2,3], Do-Youn Oh[1,2,3], Jeff Brown[7], Alan Lau[8], Mark J. O'Connor[8], and Yung-Jue Bang[1,2,3]

Abstract

Ataxia telangiectasia and Rad3-related (ATR) can be considered an attractive target for cancer treatment due to its deleterious effect on cancer cells harboring a homologous recombination defect. The aim of this study was to investigate the potential use of the ATR inhibitor, AZD6738, to treat gastric cancer.

In SNU-601 cells with dysfunctional ATM, AZD6738 treatment led to an accumulation of DNA damage due to dysfunctional RAD51 foci formation, S phase arrest, and caspase 3–dependent apoptosis. In contrast, SNU-484 cells with functional ATM were not sensitive to AZD6738. Inhibition of ATM in SNU-484 cells enhanced AZD6738 sensitivity to a level comparable with that observed in SNU-601 cells, showing that activation of the ATM-Chk2 signaling pathway attenuates AZD6738 sensitivity. In addition, decreased HDAC1 expression was found to be associated with ATM inactivation in SNU-601 cells, demonstrating the interaction between HDAC1 and ATM can affect sensitivity to AZD6738. Furthermore, in an *in vivo* tumor xenograft mouse model, AZD6738 significantly suppressed tumor growth and increased apoptosis.

These findings suggest synthetic lethality between ATR inhibition and ATM deficiency in gastric cancer cells. Further clinical studies on the interaction between AZD 6738 and ATM deficiency are warranted to develop novel treatment strategies for gastric cancer. *Mol Cancer Ther; 16(4); 566–77. ©2017 AACR.*

Introduction

DNA-damaging agents represent the cornerstone of cancer treatment. Rapid advances in cancer biology have identified key pathways involved in the repair of DNA damage. Although there are various types of DNA repair response pathways, repair of DNA double-strand breaks (DSB) by homologous recombination (HR) and nonhomologous end joining (NHEH) primarily influence the therapeutic efficacies of DNA-damaging agents (1–3). HR deficiency (HRD) is frequently observed in cancer cells, and unlike normal cells, DSBs are dealt with by NHEJ pathways that result in an intolerable level of genomic instability and cancer cell death.

Cancer cells with HRD have been shown to be particularly sensitive to DNA-damaging agents and PARP inhibitors (4–6), for example, responses to olaparib (a PARP inhibitor) were observed across different tumor types associated with germline *BRCA1/2* mutations (7). Olaparib has been approved in several countries for advanced ovarian cancer with germline *BRCA* mutation (7). However, cancer with a BRCA germ line mutation represents only a small proportion of all cancer cases, and in many countries, gastric cancer is still the leading cause of cancer-related death. Low ATM protein expressions, which contribute to HRD, predict response to PARP inhibitor in gastric cancer cells. A randomized phase II study in gastric cancer showed olaparib/paclitaxel is active in patients with metastatic gastric cancer that have failed first-line fluorouracil- and platinum-based therapy, and that its use was associated with greater overall survival in ATM_{low} patients (8). Therefore, targeting the DNA damage response (DDR) pathway might be a promising strategy for treating gastric cancer with a DNA damage repair pathway defect.

ATM and ATR play essential roles in DDR by facilitating connections between DNA damage sensing and DDR effectors. In addition, these factors regulate cell-cycle progression by controlling the activations of Chk1 and Chk2 (9–11). Interestingly, ATM and ATR are differentially activated by distinct types of DNA damage despite the fact that they function as compensatory partners by sharing substrates. ATM is primarily activated by DSBs, whereas ATR responds to a much broader spectrum of DNA damage, especially during DNA replication (9, 12). In addition, ATR plays a role in the G_2–M checkpoint, and thus, a

[1]Cancer Research Institute, Seoul National University, Seoul, Korea. [2]Biomedical Research Institute, Seoul National University Hospital, Seoul, Korea. [3]Department of Internal Medicine, Seoul National University College of Medicine, Seoul, Korea. [4]Rice University, Houston, Texas. [5]Department of Internal Medicine, Chung Ang University College of Medicine, Seoul, Korea. [6]Department of Internal Medicine, Seoul National University Bundang Hospital, Seongnam, Korea. [7]AstraZeneca R&D Boston, Waltham, Massachusetts. [8]AstraZeneca UK Ltd., Macclesfield, Cheshire, United Kingdom.

Note: Supplementary data for this article are available at Molecular Cancer Therapeutics Online (http://mct.aacrjournals.org/).

Corresponding Author: Seock-Ah Im, Seoul National University College of Medicine, 101 Daehak-ro, Jongno-gu, Seoul 03080, Korea. Phone: 82-2-2072-0850; Fax: 82-2-762-9662; E-mail: moisa@snu.ac.kr

doi: 10.1158/1535-7163.MCT-16-0378

p53 mutation leading to checkpoint-defective cells is lethal in the presence of ATR depletion (13, 14).

Because ATR inhibition is likely to have greater deleterious effects on cancer cells, ATR pathway components are considered promising therapeutic targets. Previous studies have demonstrated ATR inhibition is effective for treating cancers with HRD (15–17). Most importantly, ATR participates in functional interactions between repair proteins, especially ATM, during DDR (9, 12). Although a previous study indicated that an ATR inhibitor had a synergistic antitumor effect on ATM- or p53-deficient cancer cells when administered in combination with cisplatin in colorectal and lung cancer cell lines (14), the antitumor activity and underlying mechanisms of ATR inhibitor monotherapy on ATM status remain unclear. For this reason, we considered study of the antitumor effects of targeting ATR and of the underlying mechanisms involved would help elucidate the therapeutic role of AZD6738 in cancer and interactions between DDR-associated molecules. In addition, such studies could result in novel treatment strategies that increase the scope of ATR inhibitors to the broader HRD cancer patient population.

Although gastric cancer is rarely associated with BRCA mutation, about 14% of patients show low ATM expression and about 10% show high microsatellite instability levels, which are associated with defective DNA damage repair (8, 18). In addition, the genomes of several gastric cancer cells are modulated by epigenetic alterations that can regulate DNA damage signaling (19–23). In the present study, we investigated the antitumor effects of an ATR inhibitor, AZD6738, *in vitro* using human gastric cancer cell lines, and an *in vivo* xenograft model. AZD6738 was found to inhibit the proliferation of gastric cancer cells with dysfunctional ATM by suppressing proliferative signaling and blocking cell-cycle progression in the S phase. Furthermore, AZD6738 disrupted HR-mediated DNA repair in sensitive cells, whereas ATR inhibition activated the ATM-Chk2 pathway to promote the repair of DNA damage induced by AZD6738 in insensitive cells with functional ATM. Although earlier this year Kwok and colleagues reported that ATR inhibition is selectively sensitive to *TP53*- or *ATM* deficiency in chronic lymphocytic leukemia (CLL) cells (24), it is difficult to understand the action mechanism of ATR inhibitor and the synthetic lethal interaction between ATR and ATM in solid tumors, especially in gastric cancer. This article reveals the mechanisms underlying the action of AZD6738 in gastric cancer cells and suggests a synthetic lethal interaction between ATR inhibition and ATM deficiency. In addition, our report meaningfully evaluated that ATR to ATM switch using ATR inhibitor, that is, ATR suppression, led to compensatory ATM activation. Furthermore, we also found ATM inactivation in sensitive cells was mediated by histone deacetylase 1 (HDAC1) deficiency. These results help to understand the mechanism underlying the antitumor effect of AZD6738 and provide a rationale for a clinical trial that has been initiated for treating solid tumors, including gastric cancer.

Materials and Methods

Reagents

The ATR inhibitor AZD6738 and ATM inhibitor were kindly provided by AstraZeneca, Ltd. Cisplatin and paclitaxel were obtained from Choongwoe Co., Ltd., and Samyang Genex Co., Ltd. AZD6738 was dissolved in dimethyl sulfoxide, and cisplatin and paclitaxel were dissolved in normal saline as 10 mmol/L, and subsequently serial dilution was performed for specific concentration. The structure of AZD6738 has been previously published (25).

Cell lines and cell culture

Human gastric cancer cells (SNU-1, -5, -16, -216, -484, -601, -620, -638, -668, -719, AGS, NCI-N87, MKN-45, and KATO-III) were purchased from the Korean Cell Line Bank. Identities of the cell lines were confirmed by DNA fingerprinting analysis (26). All cells were passaged for less than 6 months before use and maintained at 37°C with a 5% CO_2 atmosphere in RPMI 1640 supplemented with 10% FBS and 10 μg/mL gentamicin.

Cell growth inhibition assay

Antiproliferative effects of AZD6738 were assessed with an MTT assay as previously described (27). Cells were seeded in 96-well plates and exposed to increasing doses of AZD6738 (ranging from 0–1 μmol/L) for 5 days. Cell viability was evaluated by measuring the absorbance at 540 nm, and IC_{50} values were analyzed using SigmaPlot software [Statistical Package for the Social Sciences, Inc. (SPSS)]. The combined effects of AZD6738 and chemotherapeutic agents were assessed using the methods previously described by Chou and Talalay (28). Any synergistic effects were defined by combination index (CI) values less than 1, whereas antagonism was identified by values more than 1.

Cell-cycle analysis

The effect of AZD6738 on cell-cycle progression was evaluated using a FACS Calibur flow cytometer (BD PharMingen) by quantifying the DNA contents of the cells stained with propidium Iodide (PI) according to previously described protocols (29). The degree of apoptosis was measured using an Annexin V–binding assay in accordance with the manufacturer's instructions (BD PharMingen). For the BrdU incorporation experiments, 10 μmol/L of BrdU were added to the cells for 3 hours before harvest. The cells were then incubated with anti-BrdU antibody for 30 minutes, stained with 7-AAD, and then subjected to FACScan cytometry according to the manufacturer's protocol (BD PharMingen). The percentage of cells in the S phase was calculated by using BD FACSDIVA software (BD PharMingen).

Western blot analysis

Total cell proteins were extracted, and 20 μg proteins were separated on 5% to 15% SDS-PAGE gels as previously described (30). Primary antibodies against phosphorylated (p)-ATM (S1981), ATM, p-ATR, ATR, p-STAT3, STAT3, p-AKT, AKT, p-ERK, ERK, p-Chk1, Chk1, p-Chk2, Chk2, p-p53, p53, p21, Mre11, XRCC1, TS, caspase-3, and cyclin E were acquired from Cell Signaling Technology. Antibodies against HDAC1, p-histone H2A.X (Millipore), PARP (BD Biosciences), and actin (Sigma Aldrich) were also purchased.

Immunoprecipitation

HDAC1–ATM interaction was examined by immunoprecipitation. Cells were transfected with HDAC-specific siRNA or nonspecific control siRNA. After 3 days, total protein was extracted from the cells and then incubated with anti-HDAC1 or anti-IgG antibodies (negative control) and protein A/G plus agarose (Santa Cruz Biotechnology).

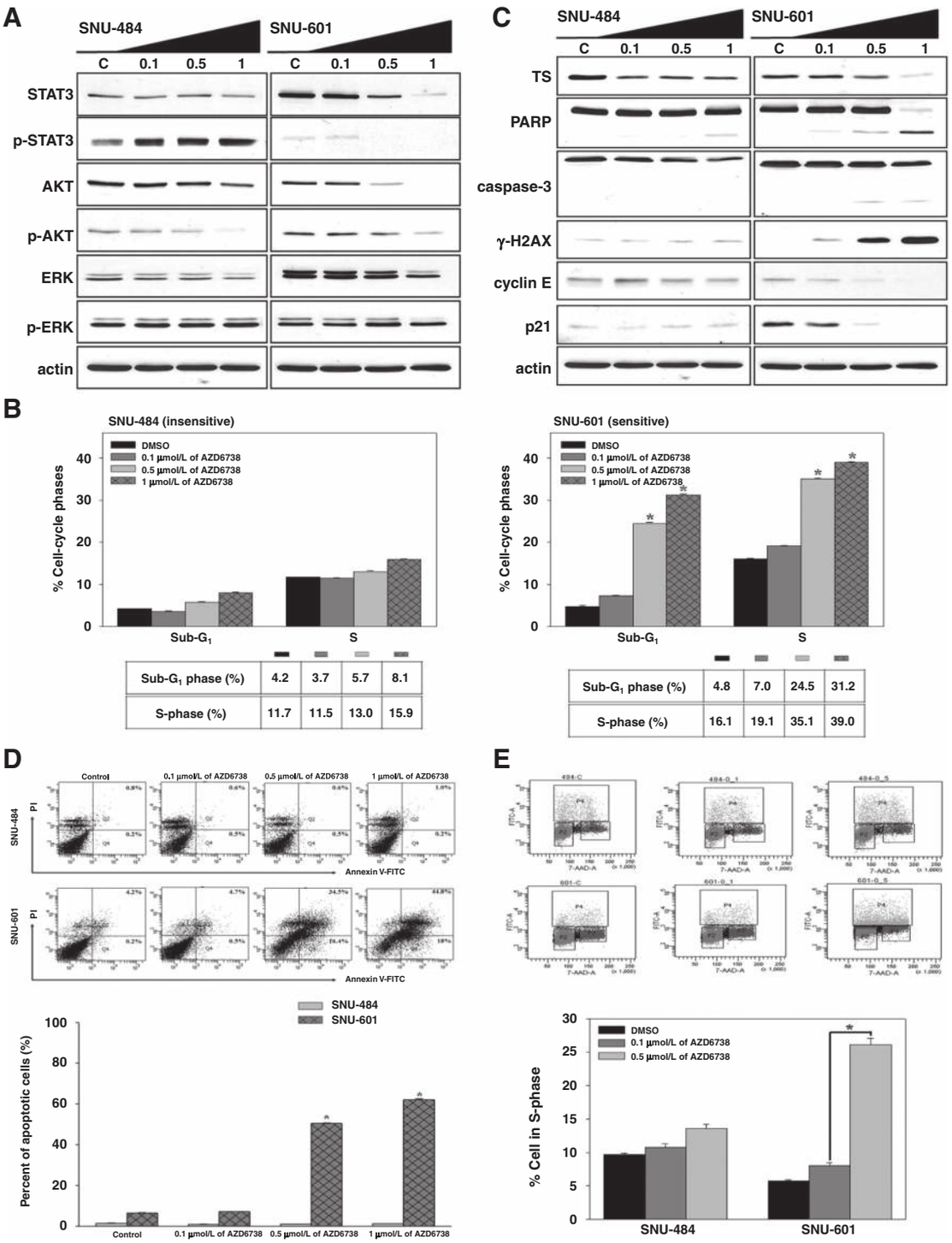

Figure 1.

AZD6738 inhibits cell proliferation. **A,** Western blotting was conducted to measure phosphorylated (p)-STAT3, (p)-AKT, and (p)-ERK levels in SNU-484 and SNU-601 cells following treatment with the indicated doses of AZD6738 for 5 days. **B,** The cells were treated with the indicated concentrations of AZD6738 for 5 days, and DNA contents were measured by FACS analysis. Populations in the sub-G_1 and S phases were calculated, and the results are presented as bar graphs with SE ($n = 3$). Columns, mean of three independent experiments; bars, ± SE; *, $P < 0.001$. **C,** The relative expression levels of cell-cycle–related proteins and γ-H2AX were measured by Western blotting following AZD6738 treatment for 5 days. **D,** The percentage of Annexin V–positive cells was determined using an Annexin V–binding assay. The numbers of early and late apoptotic cells were calculated and expressed as a bar graph. Columns, mean of three independent experiments; bars, ± SE; *, $P < 0.001$. **E,** BrdU incorporation was detected, and the percentage of cells in the S phase was calculated. Columns, mean of three independent experiments; bars, ± SE; *, $P < 0.001$.

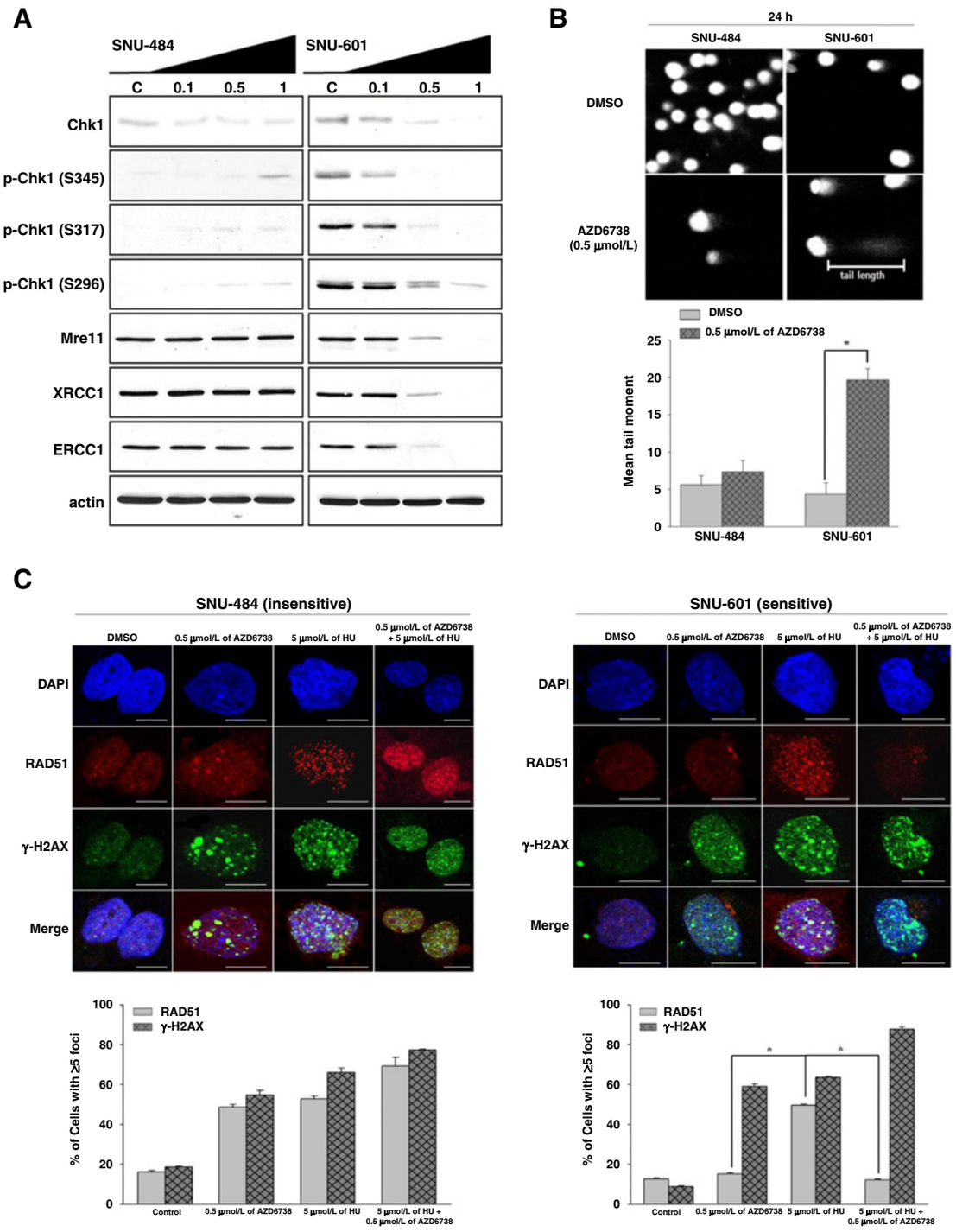

Figure 2.

AZD6738 augments DSB repair defects. **A,** Western blotting for Mre11, XRCC1, ERCC1, and p-Chk1 was performed to determine how AZD6738 affects the DDR pathway after AZD6738 treatment at the indicated concentrations for 5 days. **B,** The degree of DNA damage accumulation in individual cells was detected with an alkaline comet assay after AZD6738 or/and HU treatment for 24 hours. The degree of DNA damage accumulation was determined by evaluating the mean tail moment and is presented as a bar graph with SE ($n = 3$). **C,** An immunofluorescence assay was conducted to monitor RAD51 foci formation and determine whether DNA damage accumulation is due to a decreased HR repair capacity. The cells were exposed to AZD6738 and/or HU for 5 days, and confocal microscopy was performed to monitor the signals corresponding to RAD51 (red) and γ-H2AX (green). DAPI (blue) was used for counterstaining. Scale bars, 5 μm. The percentages of cells containing more than five RAD51 and γ-H2AX foci in three experiments are presented in a bar graph. At least 100 nuclei were analyzed for each experiment (bottom). Columns, the mean of three independent experiments; bars, ± SE; *, $P < 0.001$.

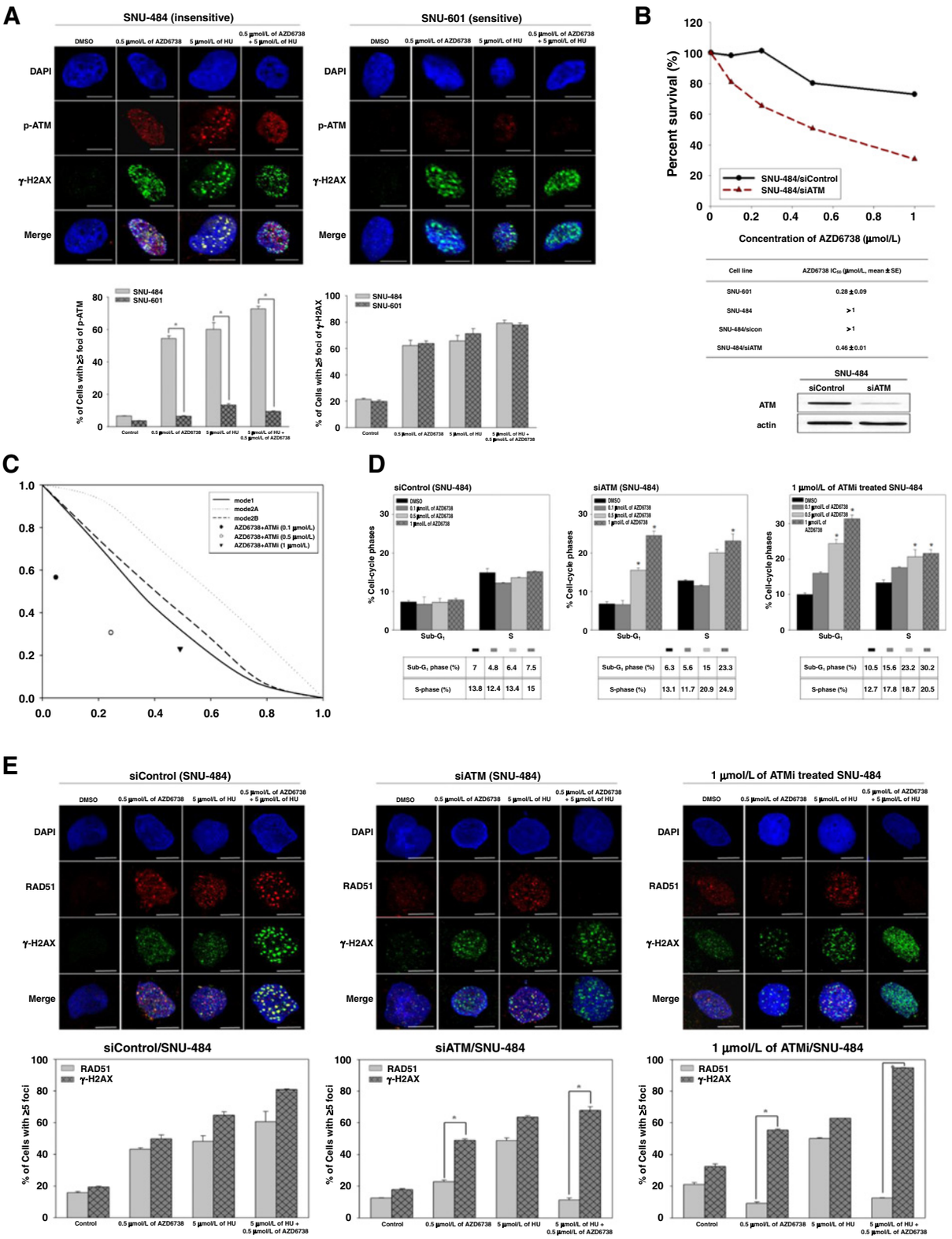

siRNA transfection

siRNA specific for ATM or HDAC1 as well as a nonspecific control was purchased from Genolution. Transfection was performed using G-fectin (Genolution) according to the manufacturer's protocol. The sequence of the ATM-specific siRNA was 5′-AACATACTACTCAAAGACATT-3′, and the sequence of the HDAC1-specific siRNA was 5′-GGCAAGUAUUAUGCUGUUATT-3′. The sequence of the nonspecific control siRNA was 5′-AATTCTCCGAACGTGTCACG-3′.

Immunofluorescence assay

An immunofluorescence assay was performed as previously described (27). The primary antibodies used for this experiment were rabbit polyclonal anti-RAD51 (H-92; Santa Cruz Biotechnology), mouse monoclonal anti–p-ATM (Cell Signaling Technology), rabbit polyclonal anti-HDAC1, and mouse monoclonal anti–p-H2A.X (Millipore) at a dilution of 1:50. The coverslips were rinsed 3 times for 10 minutes in PBS followed by incubation with the appropriate fluorophore-conjugated secondary antibody at a dilution of 1:50 (Invitrogen). The cells were counterstained with DAPI (300 nmol/L; Invitrogen), and the coverslips were mounted on slides using Faramount aqueous mounting medium (Dako). Immunofluorescence was visualized using a Zeiss LSM 510 laser scanning microscope (Carl Zeiss). At least 100 cells were analyzed for each experiment, and the ones containing more than five foci of each molecule were counted.

Comet assay

The degree of DNA damage was determined with an alkaline comet assay using a commercial kit (Trevigen) according to the manufacturer's protocol. Tail lengths were measured using the Comet assay IV program (Andor Technology).

In vivo study

Animal experiments were carried out at the animal facility of Seoul National University (Seoul, Korea) in accordance with institutional guidelines and prior approval from the Institutional Animal Care and Use Committee. A total of 10 female Balb/c athymic nude mice of 5 weeks old were purchased from Central Lab Animal, Inc., and 1×10^8 SNU-601 cells in 100 μL of PBS were injected subcutaneously into the right flank. After implantation of the tumor cells, sizes of the resulting tumors and body weight of each mouse were measured. When the tumor volume reached 200 mm^3, the mice were randomly divided into two groups (5 mice per group). One group of mice was given 50 mg/kg AZD6738 every day for 20 consecutive days via oral gavage. The control group was treated with a 10% 2-hydroxyl-propyl-β-cyclodextrine/PBS solution alone. Tumor volume was calculated using the following formula: $[(\text{width})^2 \times (\text{height})]/2$. At the end of the measurement period, the mice were euthanized with CO_2, and the tumors were excised for further analysis.

Immunohistochemistry

Immunohistochemistry and a TUNEL assay using paraffin-embedded xenograft tumor tissues were conducted as previously described (27).

Statistical analysis

All results are expressed as the mean ± SE and analyzed using SigmaPlot version 9.0 (Systat Software Inc.). A two-sided Student *t* test was performed when appropriate. *P* values <0.05 were considered statistically significant.

Results

AZD6738 inhibited the proliferation of human gastric cancer cells by inducing cell-cycle arrest and downregulating proliferative signal molecules

To assess the antiproliferative activity of AZD6738 (a novel ATR inhibitor), its growth-inhibitory effects were investigated in 14 gastric cancer cell lines using an MTT assay. The various gastric cancer cell lines showed different responses to AZD6738 (Supplementary Table S1 and Supplementary Fig. S1). SNU-601 was chosen as a sensitive cell line and SNU-484 as a resistant cell line for further investigation. Because ATR responds to various types of DNA damage that interferes with DNA replication and plays roles in intracellular signal pathways involved in cell proliferation, we investigated the downregulation of proliferative signaling after treating cells AZD6738 (11, 31). In sensitive SNU-601 cells, ATR inhibition dose-dependently induced the downregulations of proliferative signaling molecules, including AKT, STAT3, and ERK. In contrast, AKT, STAT3, and ERK were not influenced by ATR inhibition in insensitive SNU-484 cells (Fig. 1A).

ATR signaling activates downstream pathways that control cell-cycle arrest during the S to G_2 phase transition (32). Therefore, we investigated how ATR inhibition affects the cell-cycle progression of gastric cancer cells by FACS analysis. The S and sub-G_1 populations of SNU-601 cells were dramatically and dose-dependently increased by AZD6738 (Fig. 1B), and increased levels of

Figure 3.

AZD6738 exhibits a synthetic lethal interaction with ATM deficiency. **A,** The distribution and expression of p-ATM were measured with an immunofluorescence assay after AZD6738 or/and HU treatment for 5 days. Cells with more than five foci of p-ATM were counted, and the results are presented in a bar graph with SE ($n = 3$). At least 100 nuclei were analyzed for each experiment. Columns, the mean of three independent experiments; bars, ±SE; *, $P < 0.001$. **B,** ATM depletion restored AZD6738 sensitivity in SNU-484 cells. The cells were transfected with ATM-specific or nonspecific control siRNA and treated with AZD6738 for 5 days. Cell viability was measured with an MTT assay. Successful knockdown of ATM expression was evaluated by Western blotting (bottom). **C,** Dual inhibition of ATM and ATR produced a synergistic effect in SNU-484 cells. The cells were exposed to increasing doses of AZD6738 with fixed concentrations of the ATM inhibitor for 5 days. Cell viability was determined using an MTT assay. The envelopes of addictivity surrounded by solid (-), dashed (—), and dotted lines (. . .) were constructed based on the dose-response curves. **D,** ATM depletion using ATM-specific siRNA or an ATM inhibitor enhanced AZD6738-induced S arrest and apoptosis. The treated cells were exposed to the indicated concentrations of AZD6738 for 5 days, and the cell-cycle distribution was analyzed by FACS. Columns, the mean of three independent experiments; bars, ± SE; *, $P < 0.001$. **E,** SNU-484 cells transfected with nonspecific control or ATM-specific siRNA, or treated 1 μmol/L of an ATM inhibitor were exposed to AZD6738 and/or HU for 5 days. Signals corresponding to RAD51 (red) and γ-H2AX (green) were detected with microscopy. Scale bars, 5 μm. The percentages of cells with more than five foci of each molecule per 100 nuclei were determined and are presented in a bar graph. Columns, the mean of three independent experiments; bars, ± SE; *, $P < 0.001$.

cleaved PARP and caspase-3 along with γ-H2AX expression were consistent with FACS data. Inhibition of cell-cycle progression by AZD6738 also led to the downregulation of thymidylate synthase (TS), cyclin E, and p21 expression in SNU-601 cells (Fig. 1C). To confirm these observations, we evaluated percentages of apoptotic and BrdU-positive cells. The percentage of Annexin V–positive SNU-601 cells (indicating apoptotic death) was significantly increased by AZD6738 treatment (Fig. 1D) as was the percentage of cells in the S phase, whereas these increases were not observed in SNU-484 cells (Fig. 1E). These results indicated cell-cycle arrest, and the downregulations of proliferation signal pathways underlie the increased cell death shown by AZD6738-sensitive cells.

AZD6738 sensitivity was the result of reduced HR repair efficiency in AZD6738-induced DSBs

Because ATR is an essential component of HR repair, we hypothesized that ATR inhibition leads to reduced HR repair capacity and an accumulation of DNA damage. The overall expression of DDR-associated proteins was downregulated by ATR inhibition in SNU-601 cells (Supplementary Fig. S2A; Fig. 2A). Furthermore, DNA damage accumulation was also observed in SNU-601 cells treated with AZD6738, whereas no changes of DNA damage accumulation were observed in AZD6738-treated SNU-484 cells (Supplementary Fig. S2B; Fig. 2B). To verify whether DNA damage accumulation was caused by defective HR repair due to the inhibition of ATR activation, an immunofluorescence assay was used to assess RAD51 foci formation, which is indicative of functional HR repair activity. Numbers of RAD51 foci in SNU-601 cells were significantly lower than in insensitive SNU-484 cells, although degrees of DNA damage caused by hydroxyurea (HU) were comparable (Supplementary Fig. S2C; Fig. 2C). These observations support our hypothesis that ATR inhibition leads to the accumulation of DNA damage resulting from HR inactivation.

Sensitivity to AZD6738 was highly associated with ATM inactivation or dysfunction

To understand why SNU-601 and SNU-484 cells differ in terms of AZD6738 sensitivity, we focused on the expression of p-Chk1 (Supplementary Fig. S2A; Fig. 2A). Although Chk1 was not activated, DNA damage did not accumulate in AZD6738-treated SNU-484 cells. Because ATM and ATR share a number of substrates, including p53, and function in a complementary manner (10, 11, 13, 33), we examined the protein expressions of ATM-Chk2 pathway factors. ATM-Chk2 axis protein expressions were downregulated in SNU-601 cells, but the axis was activated to repair the DNA damage induced by AZD6738 in SNU-484 cells (Supplementary Fig. S3; Fig. 3A). Conversely, ATM could not be activated in SNU-601 cells, even when DNA damage was induced by irradiation (Supplementary Fig. S4).

To determine AZD6738 sensitivity was a direct result of ATM inactivation, we measured the viability of ATM-depleted SNU-484 cells treated with AZD6738. ATM knockdown using siRNA and ATM inhibition using an ATM inhibitor enhanced AZD6738 sensitivity in SNU-484 cells (Fig. 3B and C, and Supplementary Fig. S5). AZD6738-induced apoptosis and S phase cell-cycle arrest were increased in cells with siRNA-mediated or chemically downregulated ATM compared with cells transfected with control siRNA (Fig. 3D). Furthermore, the number of RAD51 foci in ATM-defective cells was significantly reduced at sites of DNA damage (Fig. 3E). Our results show ATM deficiency or inactivation might be a predictive marker for AZD6738 sensitivity in gastric cancer cells.

ATM inactivation was highly correlated with HDAC1 deficiency

Previous studies have suggested HDAC1 plays a major role in ATM activation and expression (22, 23), and HDAC1 depletion is known to suppress HR repair by inducing ATM inactivation (23, 34). To explain why ATM is inactivated in SNU-601 cells, despite unaffected total ATM levels, we examined HDAC1 expression levels in SNU-601 and SNU-484 cells. HDAC1 expression was much lower in SNU-601 cells compared with SNU-484 cells (Fig. 4A). To determine whether HDAC1 silencing enhanced AZD6738 sensitivity by modulating ATM activation, we measured the viability of siRNA-transfected HDAC1-depleted SNU-484 cells treated with AZD6738 using an MTT assay. HDAC1 knockdown was found to restore AZD6738 sensitivity in SNU-484 cells (Fig. 4B). In addition, we found that HDAC1 expression was inversely correlated with sensitivity to AZD6738 in gastric cancer cells (Supplementary Fig. S6). Furthermore, IFA assays showed HDAC1 colocalized with p-ATM in SNU-484 cells, and that HDAC1 knockdown significantly reduced p-ATM expression (Fig. 4C). An immunoprecipitation assay confirmed interaction between HDAC1 and ATM (Fig. 4D). These results indicate HDAC1 deficiency leads to ATM inactivation and AZD6738 sensitivity.

AZD6738 significantly inhibited tumor growth in an *in vivo* mouse xenograft model

To determine whether inhibition of ATR effectively inhibits *in vivo* tumor growth, we utilized a SNU-601 xenograft model. The tumor volumes in mice administered AZD6738 (50 mg/kg daily) were significantly smaller than in vehicle control (Fig. 5A), and at this dose, AZD6738 was well tolerated (Fig. 5B). Furthermore, Ki-67 expression (an indicator of proliferation) was lower in AZD6738-treated mice than in non-treated controls, indicating lower proliferative ability in AZD6738 treated mice, and TUNEL assay showed AZD6738 also increased numbers of apoptotic cells (Fig. 5C). These results were confirmed by observations of reduced expressions of proteins related to proliferation and of increased PARP cleavage following AZD6738 treatment (Fig. 5D). These findings reinforce the notion that ATR inhibition significantly suppresses cell proliferation and promotes apoptosis *in vivo*.

AZD6738 sensitized cancer cells to chemotherapeutic agents

Because platinum and 5-fluorouracil are commonly used as a first-line chemotherapy and weekly paclitaxel as a second-line chemotherapy for gastric cancer, we hypothesized that the inhibition of ATR by AZD6738 might enhance the efficacies of cytotoxic chemotherapeutics. Possible synergistic interactions between AZD6738 and paclitaxel or cisplatin were examined according to the Chou–Talalay median effect principle (28, 35). As was expected, AZD6738 sensitized some gastric cancer cells to cisplatin and/or paclitaxel (Tables 1A and 1B), which suggests AZD6738 has therapeutic potential alone and in combination with established chemotherapeutics.

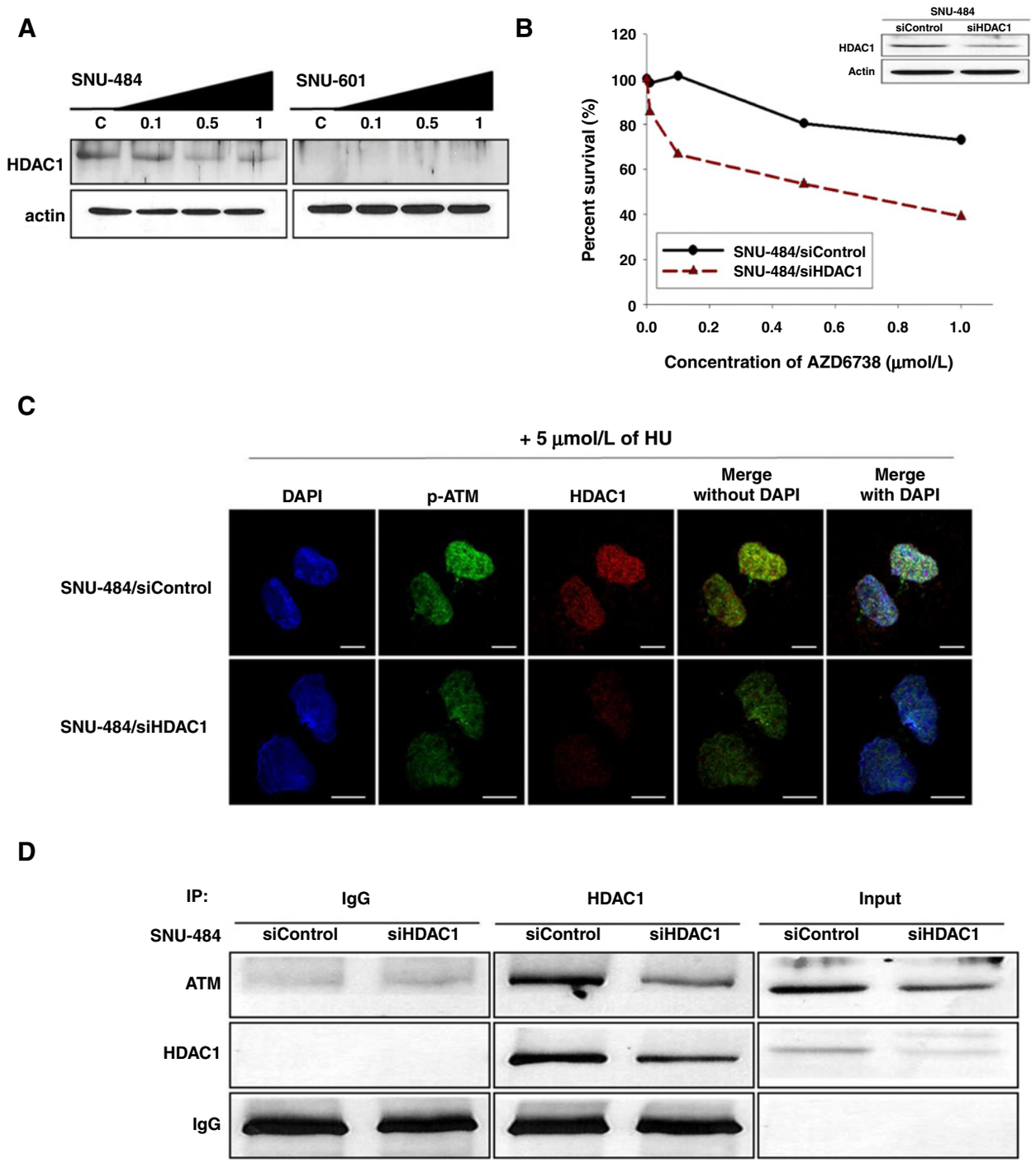

Figure 4.

HDAC1 deficiency attenuates ATM activation. **A,** The protein expression of HDAC1 was measured by Western blotting. **B,** HDAC1-specific or nonspecific control siRNA was used to transfect SNU-484 cells, and the response to AZD6738 was evaluated with an MTT assay. Reduced HDAC1 expression caused by siRNA transfection was verified by Western blotting. **C,** An immunofluorescence assay was conducted to examine the interaction of p-ATM and HDAC1. HDAC1 knockdown led to decreased p-ATM expression. Scale bars, 5 μm. **D,** SNU-484 cells were transfected with nonspecific or ATM-specific siRNA. Proteins were extracted, and immunoprecipitation was performed with anti-HDAC1 antibody. The complexes were washed in lysis buffer containing 300 mmol/L NaCl and analyzed by Western blotting using anti-HDAC1 and anti-ATM antibodies. Immunoprecipitation with an anti-IgG antibody as a negative control was also performed.

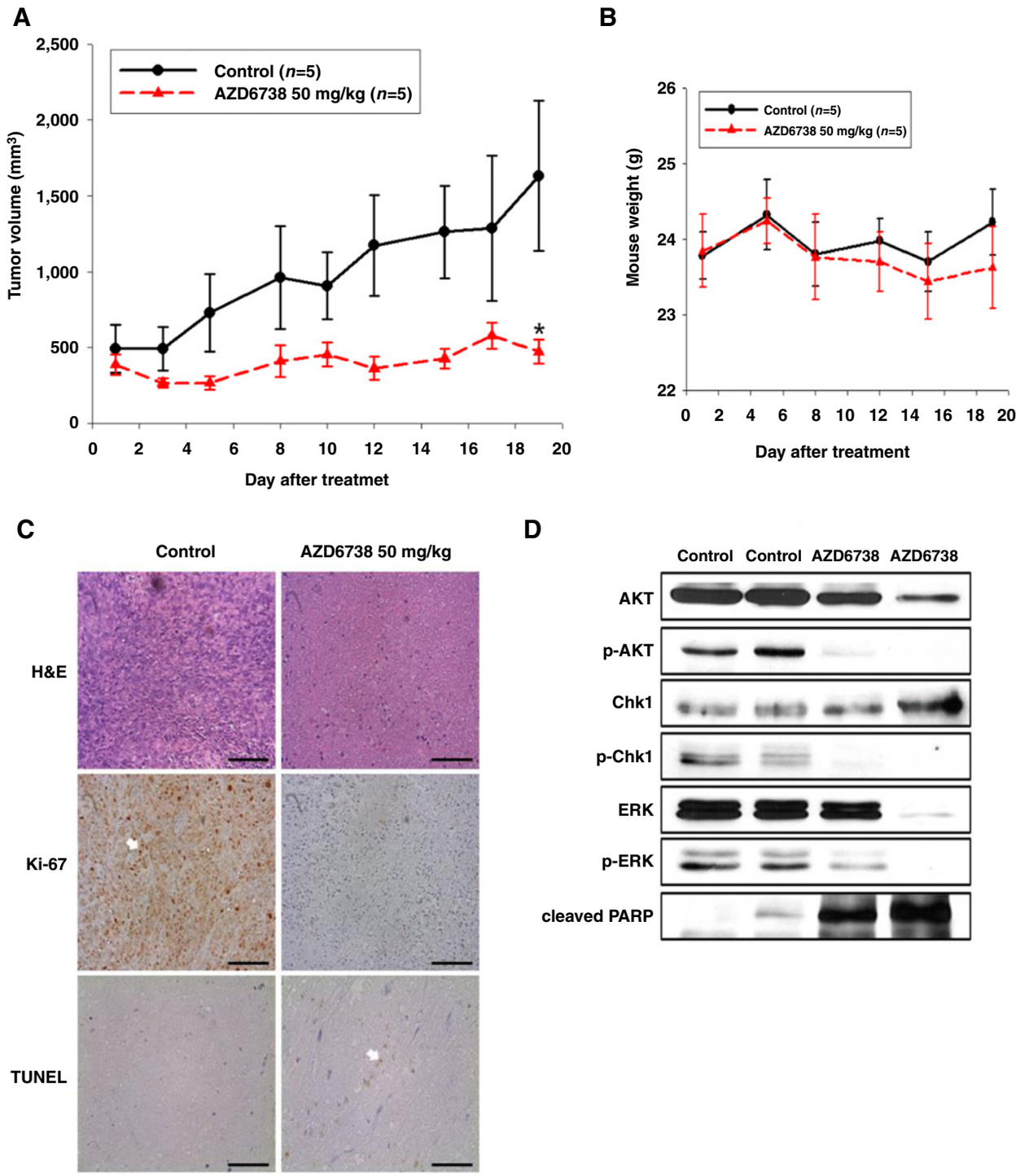

Figure 5.

AZD6738 exerts antitumor effects in a SNU-601 xenograft mouse model. **A,** Tumors formed by SNU-601 cells were grown in nude mice. The mice were treated with 50 mg/kg AZD6738 ($n = 5$) or vehicle alone ($n = 5$) daily for 20 days after the tumor volume reached 200 mm^3. The tumor volumes were measured 3 times per week using calipers and are presented as a bar graph with SE. AZD6738 impeded tumor growth in the xenograft mice compared with the control animals (*, $P < 0.001$). **B,** To detect toxicity associated with AZD6738 treatment, the body weight of each mouse was measured twice weekly. Bars, ± SE. **C,** Pathologic examination was conducted using immunohistochemical staining for Ki-67, hematoxylin and eosin (H&E) staining, and a TUNEL assay. Representative images from this study are presented, and arrows indicate positive signals (magnification, x400). Scale bars, 25 μm. **D,** Western blotting was conducted using total proteins extracted from mouse tissues to measure the expression of molecules associated with proliferation and apoptosis.

Table 1A. AZD6738 sensitizes gastric cancer cells to a DNA-damaging agent

Cell line	AZD6738 IC_{50} (μmol/L, mean ± SD)	Cisplatin IC_{50} (μmol/L, mean ± SD)	1:10 Combination IC_{50} (μmol/L, mean ± SD)	CI (ED_{50})
SNU-1	0.73	2.01 ± 0.03	0.2 ± 0.003	>1
SNU-5	>1	1.83 ± 0.05	0.19 ± 0.01	>1
SNU-16	0.8	2.21 ± 0.12	0.17 ± 0.01	>1
SNU-216	>1	4.05 ± 0.48	0.37 ± 0.1	>1
SNU-484	>1	0.83 ± 0.00001	0.06 ± 0.0007	>1
SNU-601	0.38 ± 0.03	0.59 ± 0.004	0.02 ± 0.00001	>1
SNU-620	>1	2.75 ± 0.02	0.211 ± 0.005	>1
SNU-638	0.35 ± 0.021	2.75 ± 0.07	0.13 ± 0.002	>1
SNU-668	0.83 ± 0.02	>10	0.32 ± 0.03	<1
SNU-719	>1	>10	0.18 ± 0.003	<1
AGS	0.75	1.46 ± 0.02	0.16 ± 0.004	>1
KATO-3	0.65 ± 0.02	2.07 ± 0.03	0.19 ± 0.007	<1
MKN-45	>1	>10	0.39 ± 0.3	<1
NCI-N87	0.47 ± 0.05	1.33 ± 0.006	0.063 ± 0.0002	<1

Discussion

Because ATM and ATR are essential regulators of responses to DNA damage including DSBs and replication stress, techniques for targeting ATM and ATR using highly selective small-molecule inhibitors are currently under preclinical and clinical development. In preclinical studies, many efforts have been made to identify the marker, exhibits synthetic lethal interaction with ATR inhibitors (15, 17, 24, 36). Recent reports have suggested that ATR inhibitors are effective in cells with impaired HR activities due to p53 or ERCC1 deficiency (15, 36). Although ATR inhibition is selectively effective in HR-defective cancers, malignancies lacking specific markers of HR deficiency represent only a small proportion of cancers. Furthermore, the effects of ATR inhibitors in solid tumors, including gastric cancer, and underlying mechanisms are not fully understood, and thus, there is an urgent need to evaluate the effects of ATR inhibitors on gastric cancer. In the current study, we assessed the antitumor effects of an ATR inhibitor, AZD6738, on gastric cancer cells and in a xenograft mouse model. We also explored whether ATR inhibition could increase the effectiveness of the chemotherapeutic agents used to treat gastric cancer. The results of this study might aid the selection of combinatorial regimens containing an ATR inhibitor, and present a strong rationale for conducting clinical trials in gastric cancer.

In a previous study, we found that gastric cancer cells exhibited heterogeneous responses to a PARP inhibitor and exhibited different DDR abilities (27). Although both ATR and PARP inhibitors target HR-defective cancer, the gastric cancer cell lines evaluated in both present and previous studies responded differently to these inhibitors, suggesting ATR and PARP are inhibited by different mechanisms. The antitumor effects of PARP inhibitors are based on the increased levels of genomic instability genomic instability due to DSBs induced by SSB accumulations, whereas those of ATR inhibitors are due to DNA damage accumulation due to replication stress. Because high replication stress is a characteristic of cancer, it would appear ATR inhibitor monotherapy is likely to be more effective than PARP inhibitor monotherapy. According to our data, gastric cancer cell lines exposed to ATR inhibitor in short term showed a greater antiproliferative effect than those exposed to PARP inhibitor. Moreover, unlike PARP inhibitor, ATR inhibitor directly downregulates DDR molecules, such as, Chk1, Mre11, and ERCC1, which eventually leads to the creation of cells mimicking the HR-deficient phenotype and resulting in accumulation of genomic instability.

Interestingly, in the present study, we observed that the ATM-Chk2 signaling pathway was activated when ATR activity was blocked in insensitive cells. ATM and ATR have been reported to play critical roles in DDR with overlapping functions in a partnership- and time-dependent manner (11), but

Table 1B. AZD6738 sensitizes gastric cancer cells to an anti-microtubule agent

Cell line	AZD6738 IC_{50} (μmol/L, mean ± SD)	Paclitaxel IC_{50} (μmol/L, mean ± SD)	100:1 Combination IC_{50} (μmol/L, mean ± SD)	CI (ED_{50})
SNU-1	0.73	>0.01	0.12 ± 0.008	<1
SNU-5	>1	0.005	0.63 ± 0.1	>1
SNU-16	0.8	0.0029 ± 0.0007	0.2 ± 0.03	>1
SNU-216	>1	>0.01	>1	>1
SNU-484	>1	0.0022 ± 0.0001	0.34 ± 0.08	>1
SNU-601	0.38 ± 0.02	0.004 ± 0.001	0.14 ± 0.006	<1
SNU-620	>1	0.005 ± 0.0013	0.4 ± 0.1	>1
SNU-638	0.35 ± 0.019	0.002 ± 0.0002	0.18 ± 0.005	>1
SNU-668	0.83 ± 0.028	>0.01	0.6	>1
SNU-719	>1	>0.01	0.5 ± 0.02	<1
AGS	0.75	0.004 ± 0.0005	0.21 ± 0.014	<1
KATO-3	0.65 ± 0.02	0.004 ± 0.0028	0.31 ± 0.01	>1
MKN-45	>1	>0.01	>1	>1
NCI-N87	0.47 ± 0.05	0.007 ± 0.005	0.3 ± 0.04	>1

their cross-regulation of the ATM-Chk2 and ATR-Chk1 pathways is very rare. However, a switch from ATM to ATR signaling and of Chk2 phosphorylation by ATR have been reported (12, 37, 38), and suggest that attenuated ATM activation potentiates ATR activation. Based on these reports, it is evident ATM and ATR function in a reciprocal manner, which is in-line with our result that ATR suppression promotes repair of DNA damage via ATM activation. Therefore, when ATM activation is impaired, ATM cannot adequately repair the DNA damage induced by ATR inhibition and results in cell death. This study also shows that the correlation between ATM activity, which was evaluated in gastric cancer cell lines by Kubota and colleagues (39), and the sensitivity of ATR inhibitor is statically significant and biologically meaningful (Supplementary Fig. S7). Our data indicate ATR inhibition has a synthetic lethal interaction with ATM deficiency, and that the presence of dysfunctional ATM might predict gastric cancer cell sensitivity to AZD6738. Interestingly, ATM is one of the most frequently mutated kinases in human cancers (40), and genetic alterations in *ATM* have been reported 12.2% of 287 gastric tumor samples (21), and low ATM expression has been reported in 14% of gastric cancer patients (8). The lethal effect of AZD6738 in the presence of ATM deficiency indicates ATR inhibition offers the possibility of highly attractive, effective therapeutic strategy for gastric cancer with ATM deficiency.

Recent studies have reported HDACs are involved in DDR by regulating the expressions of HR repair–associated genes (41, 42). In particular, HDACs play a critical role in mitigating ATM pathway response to DNA damage, because ATM is a substrate of HDAC (22, 23, 34). Furthermore, functional ATM activation was detected in SNU-484 cells, and not in SNU-601 cells, after IR-induced DNA damage, and it has been demonstrated HDAC1 regulates ATM activity and that HDAC1 depletion is sufficient to modulate ATM activation in response to DNA damage (22, 23, 41). These reports support our result that HDAC1 deficiency led to ATM inactivation and lethality when ATR was inhibited. HDAC1 is a well-known target of enhancer of zeste homolog 2 (Ezh2), and Ezh2 downregulation increases HDAC1 expression levels in gastric cancer. In addition, high levels of Ezh2 are frequently observed in gastric cancer tissues, and SNU-601 cells produce high levels of Ezh2 (43). These observations suggest HDAC1 depletion is caused by epigenetic modulation associated with high levels of Ezh2 expression. These results hint at a new cancer treatment strategy involving the administration of ATR inhibitor in combination with HDAC inhibitors. During our studies, we also observed the antitumor effect of AZD6738 in combination with SAHA in gastric cancer cells (data not shown). However, HDAC inhibition using small-molecule inhibitors affects numerous DNA repair factors involved at multiple levels of DNA repair pathways, and thus, side effects on normal tissues should be considered before using this combination. Taken together, our results show HDAC1 deficiency modulates ATM activity and confers sensitivity to AZD6738-induced DNA damage.

This is first study to evaluate the antitumor effects of AZD6738 on human gastric cancer cells and in a mouse model. Our findings suggest ATM activation is the main mechanism of resistance to AZD6738 and show ATM and ATR act in a compensatory manner. The study also demonstrates that AZD6738 attenuates ATR activity and induces ATM activation, and thus, promotes an ATR to ATM switch in the presence of DNA damage. These findings show the interaction between AZD6738 has a synthetic lethal interaction with ATM defect in gastric cancer cells and that ATM inactivation in ATM dysfunctional SNU-601 cells is due to HDAC1 deficiency. We believe that our findings have potential clinical implications for the treatment of ATM-defective gastric cancer, increase understanding of the mechanisms governing the action of AZD6738 alone and in combination with chemotherapeutics, and provide a rationale for present and future clinical trials.

Disclosure of Potential Conflicts of Interest

S.-A. Im is a consultant/advisory board member for AstraZeneca, Novartis, Hanmi, and Spectrum. Y.-J. Bang is a consultant/advisory board member for AstraZeneca. No potential conflicts of interest were disclosed by the other authors.

Authors' Contributions

Conception and design: A. Min, S.-A. Im, K.-H. Lee, D.-Y. Oh, J. Brown, A. Lau, M.J. O'Connor, Y.-J. Bang

Development of methodology: A. Min, S.-A. Im, K.-H. Lee

Acquisition of data (provided animals, acquired and managed patients, provided facilities, etc.): A. Min, S.-A. Im, H. Jang, H.-J. Kim

Analysis and interpretation of data (e.g., statistical analysis, biostatistics, computational analysis): A. Min, S.-A. Im, Y. Yang, K.-H. Lee, D.-Y. Oh, A. Lau, Y.-J. Bang

Writing, review, and/or revision of the manuscript: A. Min, S.-A. Im, D.K. Kim, Y. Yang, K.-H. Lee, J.W. Kim, T.-Y. Kim, J. Brown, A. Lau, Y.-J. Bang

Administrative, technical, or material support (i.e., reporting or organizing data, constructing databases): A. Min, H. Jang, S. Kim, D.K. Kim, H.-J. Kim, J. Brown

Study supervision: S.-A. Im, T.-Y. Kim, Y.-J. Bang

Other (assisted the experiment, especially performed *in vivo* experiment and also wrote and reviewed the article): M. Lee

Acknowledgments

The ATR inhibitor AZD6738 and ATM inhibitor were kindly provided by AstraZeneca, Ltd.

Grant Support

This research was supported by the Basic Science Research Program through the National Research Foundation of Korea (NRF) funded by the Ministry of Science, ICT, and Future Planning (2015R1A2A2A01004655; to S.-A. Im). This work was also funded by Basic Science Research Program through the National Research Foundation of Korea(NRF) funded by the Ministry of Science, ICT & Future Planning(2014R1A1A3052365; to H.-J. Kim). We thank to AstraZeneca for supporting this study through AZ-KHIDI Oncology Research Program.

The costs of publication of this article were defrayed in part by the payment of page charges. This article must therefore be hereby marked *advertisement* in accordance with 18 U.S.C. Section 1734 solely to indicate this fact.

Received June 14, 2016; revised November 1, 2016; accepted December 8, 2016; published OnlineFirst January 30, 2017.

References

1. Lord CJ, Ashworth A. Mechanisms of resistance to therapies targeting BRCA-mutant cancers. Nat Med 2013;19:1381–8.

2. Pitroda SP, Pashtan IM, Logan HL, Budke B, Darga TE, Weichselbaum RR, et al. DNA repair pathway gene expression score correlates with repair

proficiency and tumor sensitivity to chemotherapy. Sci Transl Med 2014;6: 229ra242.
3. Madhusudan S, Middleton MR. The emerging role of DNA repair proteins as predictive, prognostic and therapeutic targets in cancer. Cancer Treat Rev 2005;31:603–17.
4. Fong PC, Boss DS, Yap TA, Tutt A, Wu P, Mergui-Roelvink M, et al. Inhibition of poly(ADP-ribose) polymerase in tumors from BRCA mutation carriers. N Engl J Med 2009;361:123–34.
5. O'Sullivan CC, Moon DH, Kohn EC, Lee JM. Beyond breast and ovarian cancers: PARP inhibitors for BRCA mutation-associated and BRCA-like solid tumors. Front Oncol 2014;4:42.
6. Abdel-Fatah TMA, Arora A, Moseley P, Coveney C, Perry C, Johnson K, et al. ATM, ATR and DNA-PKcs expressions correlate to adverse clinical outcomes in epithelial ovarian cancers. BBA Clin 2014;2:10–7.
7. Kaufman B, Shapira-Frommer R, Schmutzler RK, Audeh MW, Friedlander M, Balmana J, et al. Olaparib monotherapy in patients with advanced cancer and a germline BRCA1/2 mutation. J Clin Oncol 2015; 33:244–50.
8. Bang YJ, Im SA, Lee KW, Cho JY, Song EK, Lee KH, et al. Randomized, double-blind phase II trial with prospective classification by ATM protein level to evaluate the efficacy and tolerability of olaparib plus paclitaxel in patients with recurrent or metastatic gastric cancer. J Clin Oncol 2015; 33:3858–65.
9. Adams BR, Golding SE, Rao RR, Valerie K. Dynamic dependence on ATR and ATM for double-strand break repair in human embryonic stem cells and neural descendants. PLoS One 2010;5:e10001.
10. Goodarzi AA, Block WD, Lees-Miller SP. The role of ATM and ATR in DNA damage-induced cell cycle control. Prog Cell Cycle Res 2003;5:393–411.
11. Weber AM, Ryan AJ. ATM and ATR as therapeutic targets in cancer. Pharmacol Ther 2015;149:124–38.
12. Saha J, Wang M, Cucinotta FA. Investigation of switch from ATM to ATR signaling at the sites of DNA damage induced by low and high LET radiation. DNA Repair 2013;12:1143–51.
13. Pabla N, Huang S, Mi QS, Daniel R, Dong Z. ATR-Chk2 signaling in p53 activation and DNA damage response during cisplatin-induced apoptosis. J Biol Chem 2008;283:6572–83.
14. Reaper PM, Griffiths MR, Long JM, Charrier JD, Maccormick S, Charlton PA, et al. Selective killing of ATM- or p53-deficient cancer cells through inhibition of ATR. Nat Chem Biol 2011;7:428–30.
15. Mohni KN, Kavanaugh GM, Cortez D. ATR pathway inhibition is synthetically lethal in cancer cells with ERCC1 deficiency. Cancer Res 2014;74: 2835–45.
16. Fokas E, Prevo R, Pollard JR, Reaper PM, Charlton PA, Cornelissen B, et al. Targeting ATR in vivo using the novel inhibitor VE-822 results in selective sensitization of pancreatic tumors to radiation. Cell Death Dis 2012;3:e441.
17. Menezes DL, Holt J, Tang Y, Feng J, Barsanti P, Pan Y, et al. A synthetic lethal screen reveals enhanced sensitivity to ATR inhibitor treatment in mantle cell lymphoma with ATM loss-of-function. Mol Cancer Res 2015;13:120–9.
18. Kim JW, Im SA, Kim MA, Cho HJ, Lee DW, Lee KH, et al. Ataxia-telangiectasia-mutated protein expression with microsatellite instability in gastric cancer as prognostic marker. Int J Cancer 2014;134:72–80.
19. Fu DG. Epigenetic alterations in gastric cancer (Review). Mol Med Rep 2015;12:3223–30.
20. Gigek CO, Chen ES, Calcagno DQ, Wisnieski F, Burbano RR, Smith MA. Epigenetic mechanisms in gastric cancer. Epigenomics 2012;4: 279–94.
21. Cancer Genome Atlas Research Network. Comprehensive molecular characterization of gastric adenocarcinoma. Nature 2014;513:202–9.
22. Goodarzi AA, Noon AT, Deckbar D, Ziv Y, Shiloh Y, Lobrich M, et al. ATM signaling facilitates repair of DNA double-strand breaks associated with heterochromatin. Mol Cell 2008;31:167–77.
23. Thurn KT, Thomas S, Raha P, Qureshi I, Munster PN. Histone deacetylase regulation of ATM-mediated DNA damage signaling. Mol Cancer Ther 2013;12:2078–87.
24. Kwok M, Davies N, Agathanggelou A, Smith E, Oldreive C, Petermann E, et al. ATR inhibition induces synthetic lethality and overcomes chemoresistance in TP53- or ATM-defective chronic lymphocytic leukemia cells. Blood 2016;127:582–95.
25. Frank PV, Alan L, Sandra S, Thomas PC, Mark JO, Christopher JB. The orally active and bioavailable ATR kinase inhibitor AZD6738 potentiates the antitumor effects of cisplatin to resolve ATM-deficient non-small cell lung cancer *in vivo*. Oncotarget 2015;6:44289–305.
26. Ku JL, Park JG. Biology of SNU cell lines. Cancer Res Treat 2005;37:1–19.
27. Min A, Im SA, Yoon YK, Song SH, Nam HJ, Hur HS, et al. RAD51C-deficient cancer cells are highly sensitive to the PARP inhibitor olaparib. Mol Cancer Ther 2013;12:865–77.
28. Chou TC. Drug combination studies and their synergy quantification using the Chou-Talalay method. Cancer Res 2010;70:440–6.
29. Min A, Im SA, Kim DK, Song SH, Kim HJ, Lee KH, et al. Histone deacetylase inhibitor, suberoylanilide hydroxamic acid (SAHA), enhances anti-tumor effects of the poly (ADP-ribose) polymerase (PARP) inhibitor olaparib in triple-negative breast cancer cells. Breast Cancer Res 2015;17:33.
30. Kang S, Min A, Im SA, Song SH, Kim SG, Kim HA, et al. TGF-beta suppresses COX-2 expression by tristetraprolin-mediated RNA destabilization in A549 human lung cancer cells. Cancer Res Treat 2015;47:101–9.
31. Hitomi M, Yang K, Stacey AW, Stacey DW. Phosphorylation of cyclin D1 regulated by ATM or ATR controls cell cycle progression. Mol Cell Biol 2008;28:5478–93.
32. Niida H, Katsuno Y, Banerjee B, Hande MP, Nakanishi M. Specific role of Chk1 phosphorylations in cell survival and checkpoint activation. Mol Cell Biol 2007;27:2572–81.
33. Smith J, Tho LM, Xu N, Gillespie DA. The ATM-Chk2 and ATR-Chk1 pathways in DNA damage signaling and cancer. Adv Cancer Res 2010;108:73–112.
34. Karagiannis TC, El-Osta A. The paradox of histone deacetylase inhibitor-mediated modulation of cellular responses to radiation. Cell Cycle 2006;5:288–95.
35. Chou TC, Talalay P. Quantitative analysis of dose-effect relationships: The combined effects of multiple drugs or enzyme inhibitors. Adv Enzyme Regul 1984;22:27–55.
36. Toledo LI, Murga M, Zur R, Soria R, Rodriguez A, Martinez S, et al. A cell-based screen identifies ATR inhibitors with synthetic lethal properties for cancer-associated mutations. Nat Struct Mol Biol 2011;18:721–7.
37. Shiotani B, Zou L. Single-stranded DNA orchestrates an ATM-to-ATR switch at DNA breaks. Mol Cell 2009;33:547–58.
38. Wang XQ, Redpath JL, Fan ST, Stanbridge EJ. ATR dependent activation of Chk2. J Cell Physiol 2006;208:613–9.
39. Kubota E, Williamson CT, Ye R, Elegbede A, Peterson L, Lees-Miller SP, et al. Low ATM protein expression and depletion of p53 correlates with olaparib sensitivity in gastric cancer cell lines. Cell Cycle 2014;13:2129–37.
40. Greenman C, Stephens P, Smith R, Dalgliesh GL, Hunter C, Bignell G, et al. Patterns of somatic mutation in human cancer genomes. Nature 2007; 446:153–8.
41. Smith S, Fox J, Mejia M, Ruangpradit W, Saberi A, Kim S, et al. Histone deacetylase inhibitors selectively target homology dependent DNA repair defective cells and elevate non-homologous end joining activity. PLoS One 2014;9:e87203.
42. Ha K, Fiskus W, Choi DS, Bhaskara S, Cerchietti L, Devaraj SG, et al. Histone deacetylase inhibitor treatment induces `BRCAness' and synergistic lethality with PARP inhibitor and cisplatin against human triple negative breast cancer cells. Oncotarget 2014;5:5637–50.
43. Choi JH, Song YS, Yoon JS, Song KW, Lee YY. Enhancer of zeste homolog 2 expression is associated with tumor cell proliferation and metastasis in gastric cancer. APMIS 2010;118:196–202.